QUANTITATIVE SURFACE MORPHOLOGY ANALYSIS USING ROUGHNESS PARAMETERS

ANALISIS CUANTITATIVO DE LA MORFOLOGÍA SUPERFICIAL USANDO LOS PARAMETROS DE RUGOSIDAD

M.P. Hernández[a†], G. Hernández[b]

a) Instituto de Ciencia y Tecnología de Materiales (IMRE), Universidad de La Habana, Zapata y G, El Vedado, Plaza de la Revolución, La Habana 10400, Cuba; mayrap@imre.uh.cu†
b) División de Validación y Metrología (ESINES). 198 entre 17 y 19, Rpto Siboney, Playa, La Habana 11300, Cuba.
† corresponding author

Recibido 24/4/2020; Aceptado 4/3/2021

The surface morphology of CdS thin films heat treated with $CdCl_2$ after grown has been quantified from atomic force microscopy micrographs using roughness parameters: roughness average (Ra), root mean square (RMS) and maximum height of the profile (R_{p-v}). The CdS thin films were growth by Close Space Sublimation (CSS) with source temperature of the CdS (T_{Sour}) at 650°C and at four substrate temperatures (T_{Sub}): 200, 300, 350 and 450°C. The wet $CdCl_2$ treatment on CdS was preformed depositing drops of methanol solution containing $CdCl_2$ at 0.5 wt. %, blowing it with air and then letting it dry at room temperature. The results showed that the surface roughness of CdS film depended on the substrate temperature during the growth process and the $CdCl_2$ heat treatment times. The changes of the roughness were linked directly to the recrystallization process. The roughness parameters demonstrate it efficiency in the quantification of the surface morphology and excellent tool for the evaluation of the technology process.

La morfología superficial de capas delgadas de CdS policristalino crecidas y posteriormente tratadas por $CdCl_2$ ha sido cuantificada a partir de imágenes de microscopía de fuerza atómica usando los parametros de rugosidad: rugosidad promedio (Ra), raíz media cuadrática de la rugosidad (RMS) y máxima altura del perfil (R_{p-v}). Las capas delgadas de CdS se crecieron por el método de sublimación en espacio cerrado (CSS) a la temperatura de la fuente de CdS (T_{Sour}) de 650°C y a cuatro temperaturas del sustrato (T_{Sub}): 200, 300, 350 y 450°C. El tratamiento húmedo con $CdCl_2$ sobre películas delgadas de CdS se realizó depositando gotas de una solución de $CdCl_2$ al 0.5 wt. % en metanol. Los resultados mostraron que la rugosidad de la superficie de las capas delgadas de CdS dependía de la temperatura del sustrato durante el proceso de crecimiento y de los tiempos de recocido de los tratamientos con $CdCl_2$. Los cambios de la rugosidad fueron vinculados directamente al proceso de recristalización. Los parametros de rugosidad demostraron su eficiencia en la cuantificación de la morfología de la superficie y como excelente instrumento para la evaluación de procesos tecnológicos.

PACS: Acoustical properties of solid surfaces and interfaces (propiedades acústicas de interfaces y superficies sólidas), 68.35.Iv; structure and roughness of interfaces (estructura y rugosidad de interfaces), 68.35.Ct; impurities in thin films (impurezas en capas delgadas), 68.55.Ln.

I. INTRODUCTION

Quantification of the surface morphology is important to clarify a number of phenomena including adsorption on surfaces, fracture, aggregation of colloids, and electrical properties [1]. The studies on roughness evolution in thin films can lead to a better understanding of the processes themselves, perhaps even at atomistic levels.

The concept of texture is associated to the three dimensional presentation of the real surface morphology. Surface texture is the repetitive or random deviation from the nominal surface that forms the three dimensional topography of the surface. Surface texture includes the roughness (nano- and microroughness), formed by fluctuations in the surface of short wavelengths, characterized by hills (local maxima) and valleys (local minima) of varying amplitudes and spacing [2].

The roughness has statistical implications as it takes into consideration factors such as sample size and sampling interval. It is quantified by the vertical spacing of a real surface from its ideal form. If these spacing is large, the surface is rough; if it is small the surface is smooth. The roughness can be characterized, for example, by height parameters, wavelength parameters, spacing and hybrid parameters [3].

Eventually, the characterization technique of the surface involves concepts of fractal geometry, which are widely used to describe the surface morphology [4]. The fractal approach has the ability to characterize surface roughness by scale independent parameters and provides information on the roughness structure at all length scales that exhibit the fractal behavior.

The studies of surfaces provide insight into the fundamental growth dynamics and enables one to control the roughness of the films. The kinetic roughening theory has received special attention for its usefulness to studies on roughness evolution in thin films grown under far-from-equilibrium conditions [5]. Typically, roughness of a surface evolves as a consequence of simultaneous atomic scale processes such as direct addition of atoms on the growing surface from the surrounding, removal of atoms from the surface and motion of atoms along the

surface or diffusive mass transport [6].

Atomic force microscopy (AFM) has been developed to obtain a micrograph of a material surface on a molecular scale. AFM is a nondestructive imaging technique which provides three dimensional surface topographies with high information density in a digital format amenable to mathematical analysis. Surface structures are characterized on the scale of nanometers to microns. Also, the application of AFM has been extended beyond the analysis of metals and conventional semiconductors to a wide range of materials. Thus, it seems that AFM is an obvious and attractive technique for morphology analysis that can provide direct measurements of the surface.

In deposition processes used to fabricate thin solid films, there is a very sensitive and complex dependence of film microstructure on growth conditions [7]. This microstructure has a profound incidence on all physical properties (electrical, mechanical, optical, etc.) of the film [8–10].

In particular, in the polycrystalline semiconductors, the trapping of charge at the grain boundaries has a decisive influence on the electrical transport properties through the formation of electrostatic potential barriers. There is a great technological interest in polycrystalline materials because the manufacturing process is cheap and versatile. Among them are the III-V, II-VI, IV-IV compounds like GaAs, ZnO and SiC, metal oxides (TiO_2, SnO_2, $BaTiO_3$, $SrTiO_3$) or ternary ($CuInSe_2$, $Hg_{1-x}Mn_xTe$, $(BiSb)_2Te_3$), which are used in electronic devices, optic fibers, interferential filters, other applications [11–14].

CdS films have been grown using a variety of growth techniques [15–17]. Depending on the growth technique, microstructure and impurity inclusions are going to vary. Among he many heat treatment methods available, the one using a thin $CdCl_2$ coating followed by heat treatment in air is well known to greatly improve the structural and the electrical properties of CdS quality and CdS/CdTe solar cell efficiency [18–20]. The effect of chlorine treatment on CdTe solar cells is possibly the single most studied topic of the field owing to the vast array of structural and electrical changes it induces within the device.

The objective of this work is to describe the surface evolution of the as grown CdS and treated by $CdCl_2$ from the quantitative morphology analysis. The roughness parameters were calculated using AFM micrographs. The variation of the roughness provoked by the substrate temperature in the growth process and the heat treatment time the $CdCl_2$ were correlated with the grain boundary, grain size and the microstructure illustrating the importance of quantification of the surface morphology as a tool for the control of the physical properties of the films.

II. EXPERIMENTAL DETAILS

II.1. Growth thin films of CdS

The samples were prepared by CSS with a base pressure of 10^{-5} Torr using ITO glass as substrate. The raw material was CdS powder (99.99 at. % purity) from Balzers. For all thin films, the CdS source maintained the temperature at T_{Sour} = 650°C during the growth process using T_{Sub} ranging from 200 to 450°C.

The source and substrate heaters were graphite blocks. The measurements of the source and substrate temperatures were obtained by cromel-alumel thermocouple, which was placed in an orifice inside the graphite blocks. The gas used during the film growth was argon (99.999 at. % pure) from Matheson. The deposition time of the growth was 2 min.

II.2. Procedure with $CdCl_2$

15 drops of the methanol solution containing $CdCl_2$ at 0.5 wt. % are deposited on the surface of the CdS, blowing it with air and then letting it dry at room temperature. The CdS films received thermal treatments after the deposition of $CdCl_2$.

II.3. Analysis structural of CdS films

XRD analysis was used to recognize the structural phases and to evaluate the crystalline size. X-ray diffractograms were made with a Krublet diffractometer using the CuKα, radiation with λ_1 = 1.54056Å and λ_2 = 1.54439Å. A XRD patterns were recorded in the range $20° - 70°$ with a step size of 0.02°.

II.4. Analysis of the surface

Atomic Force Microscope (Auto probe CP from Park Scientific) in air operating in contact mode was used to analyze the surface morphology. Measurements were performed with Si tips. AFM micrographs were acquired outside central and border regions of the films. The micrographs processing used Nanotec WSxM 5.0 Develop 9.1 software [21]. Roughness parameters: height average ($\overline{Z}$), roughness average (*Ra*), root mean square (*RMS*) and maximum height of the profile (R_{p-v}) described the surface morphology [3].(see Appendix)

The 3D contour graphics were constructed in MathCad 7.0 software. Inside them, the (X,Y) plane corresponded to the CdS surface and the Z projection represented the roughness parameter.

III. RESULTS AND DISCUSSION

III.1. Evaluation of the surface roughness homogeneity

In order to evaluate the surface roughness homogeneity of the as grown and $CdCl_2$-treated CdS films, AFM micrographs were acquired in two radial directions, which were perpendicular to each other.

Figure 1 displays 3D contour graphics of *Ra*. Figure 1a shows the CdS films grown at T_{Sour} = 650°C and T_{sub} = 350°C and Figure 1b corresponds to the CdS films treated by 0.5 wt. %$CdCl_2$ in methanol. After, the films with $CdCl_2$ treatment was heated at 500°C for 15 min in the air. The black arrows

to the right and left of the 3D contour graphics indicate the position of the current electrodes in the graphite block and the direction of the current. The thermocouple immersed into graphite block was located on the center surface.

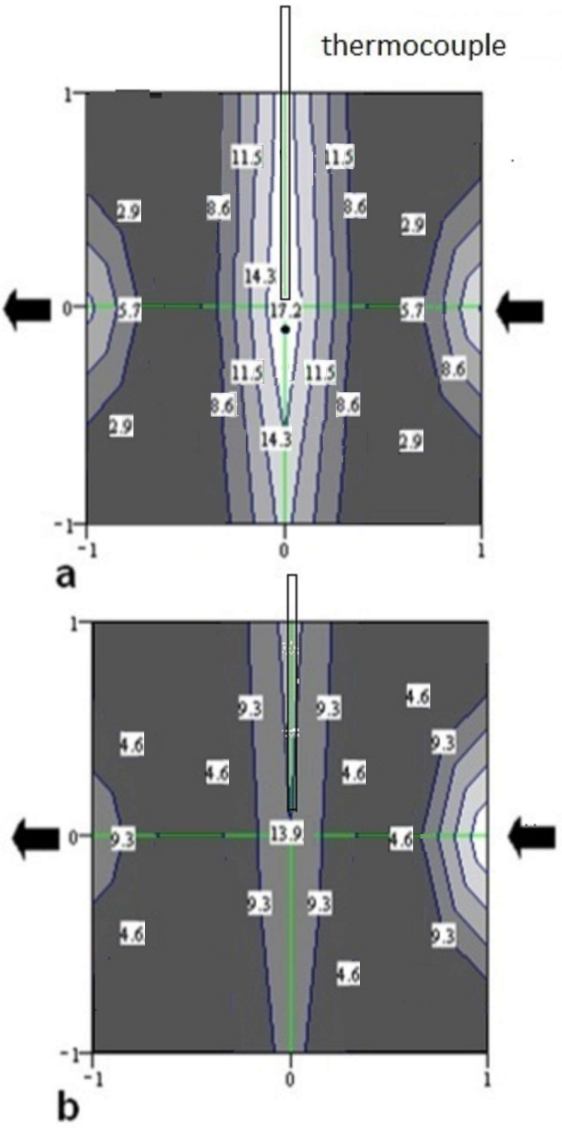

Figure 1. 3D contour graphics of the Ra parameter for : a) as grown CdS film, which grown on ITO glass slides at T_{Sour} at 650°C and T_{sub} at 350°C during 2 min; b) CdS film treated by methanol solution of the $CdCl_2$ at 0.5 wt. % and after it heated at 500°C for 15 min in the air.

In both figures (1a and 1b), the highest values of *Ra* correspond to the closure of the central region where is located in the thermocouple and near the electrodes, which is the less hot region. As a result, surface roughness inhomogeneity are observed. In order to prevent the tip from being broken, the center of scanning area is set at the point of 260 μ m away from the center in the horizontal direction.

However, the *Ra* values of the center and the border of the films decreased by $CdCl_2$ treatment, which reduced the largest *Ra* values and incremented the smaller ones, producing a slight tendency to homogeneity of the surface. This result indicated that the $CdCl_2$ treatment provoked a decreasing of the surface roughness. The process of the recrystallization and the improvement of the structural perfection and quality of CdS polycrystalline films with the $CdCl_2$ treatment have recently been reported by others [19,22,23].

III.2. Effect of the Substrate temperature on the roughness parameter

Figure 2 shows AFM micrographs of the as grown and $CdCl_2$-treated CdS films. CdS thin films were grown varying T_{Sub} at 200, 300 and 350°C. After $CdCl_2$ treatment, the films were heated at 500°C for 15 min in the air. The micrograph of the as grown CdS film shows small grains on the surface. Several authors have demonstrated the effects of source and substrate temperature, ambient gas pressure and the separation between source and substrate in CSS on surface morphology of the films [24–26]. In this work, the AFM micrographs as grown CdS films and after treatment with $CdCl_2$ indicate a progressive reduction in grain size with the substrate temperature. After $CdCl_2$ treatment, a significant change in the grain size of the CdS film was observed. The film showed large grains and a densely packed morphology. Apparently, the small grains grew by moving the grain boundaries to form large grains by effect of the $CdCl_2$. These results are known, and it has been reported by various authors [20,27].

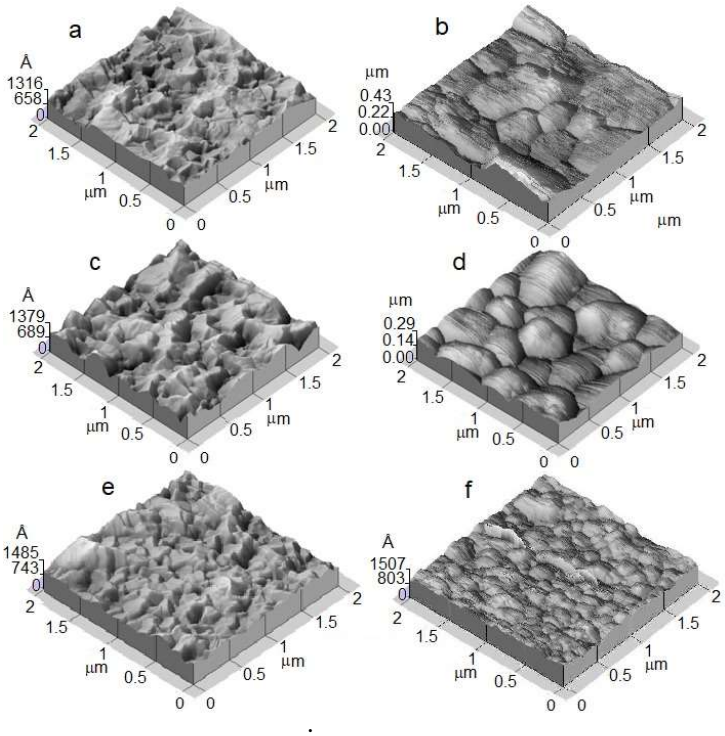

Figure 2. AFM micrographs of the CdS films grown at T_{Sour} at 650°C and T_{Sub} varied at 200, 300 and 350°C during 2 min, without (a,c,e) and with $CdCl_2$ treatment by methanol solution of the $CdCl_2$ at 0.5 wt. % and after heating substrates at 500°C for 15 min in the air(b,d,f)

The changes on surface morphology produced by substrate temperature are quantified with roughness parameters for as grown CdS films and treated by the $CdCl_2$. Table III.2 showed

drastic variation of these parameters, where can observe one abrupt reduction of the *Z*, *Ra* and *RMS* occurred with the increasing of the substrate temperature. In conclusion, the substrate temperature provoked the decreasing of the surface roughness. This behavior could be justified taking into account the strong temperature dependent of the mobilities of grain boundaries and rate of grain growth. Both factors can be used to control grain growth in films.

A comparative analysis between the roughness parameters of the as grown CdS thin films and treated by $CdCl_2$ at 350°C demonstrate that there was a slight effect of the $CdCl_2$ treatment on surface morphology. The small grains observed on the surface treated by $CdCl_2$ could indicate the beginning of the recrystallization process. This suggests that higher temperature of treatment are needed to increasing of the recrystallization. This behavior has been seen in CdTe films grown by CSS and treated by $CdCl_2$, where the films do not show changes on surface with high substrate and treatment temperatures. [28, 29].

Table 1. Surface roughness parameters for as grown CdS films (at T_{Sour} at 650°C varying T_{Sub} at 200, 300 and 350°C during 2 min) and with $CdCl_2$ treatment (0.5 wt % $CdCl_2$ in methanol and after it heated at 500°C for 15 min in the air).

	as grown CdS			**$CdCl_2$ treatment**		
(textbfT_{Sub} °C)	*Z* nm	*Ra* nm	*RMS* nm	*Z* nm	*Ra* nm	*RMS* nm
200	313 ± 12	104 ± 4	154 ± 6	134 ± 5	43.0 ± 1.6	58.1 ± 2.3
300	131 ± 5	35.4 ± 1.3	37.6 ± 1.4	103 ± 4	31.8 ± 1.4	38.5 ± 1.5
350	36.8 ± 1.5	8.8 ± 0.3	9.2 ± 0.2	34.8 ± 1.2	7.2 ± 0.3	10.6 ± 0.5

III.3. Effect of the heat treatment times after $CdCl_2$ treatment

Many works from different research groups on CdTe solar cell have reported the effect of $CdCl_2$ heat treatment, but very few are available on the importance of time evolution to the post-$CdCl_2$ heat treatment [30, 31] In this subsection, the impact of the heat treatment times on the structural and morphological of CdS thin films has been explored using a $CdCl_2$ heat treatment at vacuum with varying treatment times and followed by similar heat treatment at air to those used in the subsection (ii).

Figure 3 shows the AFM micrograph of as grown CdS films at T_{Sour}=650°C and T_{Sub} =450°C during 2 min and after treated by 0.5 wt %$CdCl_2$ in methanol. The films treated by $CdCl_2$ were heating in the reaction chamber at T=300°C at 10^{-5} Torr using variable times of the 1, 2 and 4 min. After, these films were heated at 500°C for 15 min in the air. The included histogram of the Figure 3 represent height distributions for vacuum heat times at 1, 2 and 4 min.

The micrograph of the as grown CdS film at T_{Sub} =450°C showed a very irregular surface (see Figure 3). The roughness parameters of this surface are Z =31.71 nm, Ra =7.01 nm and RMS= 9.3 nm, being slightly lower values than those reported in Table III.2.

Table III.3 parameters gives the quantification of the roughness parameters for each vacuum heat treatment times. For all times, the surface roughness for treated films are higher than without treatment. The parameters *Z*, *Ra* and *RMS*, S_{ku} and S_{sk} were influenced by the vacuum heat treatment times. The S_{sk} parameter is close to zero at 2 min indicating the most symmetric peak distribution, while that S_{ku} parameter is major than 3 suggesting broadened height distributions. The histograms of Figure 3 confirmed these behaviors.

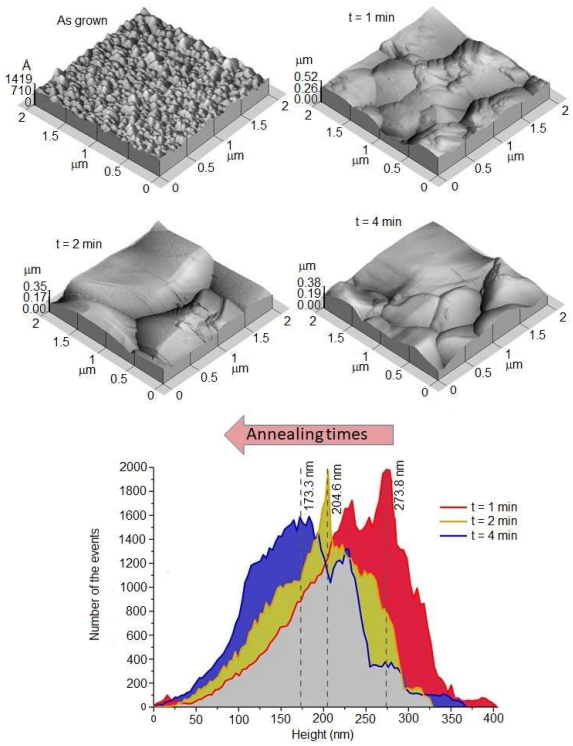

Figure 3. AFM micrographs of the CdS treated by 0.5 wt %$CdCl_2$ in methanol. After the treated films were heated in the reaction chamber at T_{Sub}=300°C at 10^{-5}Torr using treatment times (1, 2 and 4 min) and following a heat treatment at 500°C for 15 min in the air. Height distributions correspond at 1, 2 and 4 min

The combination of the heat treatment in the reaction chamber at T=300°C at 10^{-5} Torr with variable times and at 500°C for 15 min in the air modified the surface morphology provoking a drastic increasing of the roughness parameters with respect to heat treatment only in air (see Table III.2). The heat treatment avoided the impurities from air which can affect the film structure basically the grain growth. Although it is difficult to isolate it from the effects of oxygen it seems clear that $CdCl_2$ treatment is the effect dominant in the increasing of the roughness parameters [32, 33]. Nevertheless, the application of $CdCl_2$ heat treatment in the presence of oxygen is a fact that achieves the highest efficiencies of CdTe solar cell [34].

Table III.3 shows that as the vacuum heat treatment times starts rising, the parameters *Z*, *Ra* and *RMS*, decrease, and they start get up again while the times increases, being the highest values of *Z*, *Ra* and *RMS* for 1 min and the minimum value for 2 min. We correlated these results with a recrystallization process. Recrystallization consists of nucleation and growth of a new crystalline structure, with lower strain energy, at the

expense of the original crystalline structure, and is generally followed by grain growth. The driving force for this process is the high stored energy present in the crystal defects. The condition for the occurrence of the recrystallization is the favorable energy balance between the decreasing of stored energy due to the elimination of defects (rearrangement and annihilation of crystal defects) caused by the passage of the boundary and the increasing of the total grain boundary energy [35].

Table 2. Surface roughness parameters for CdS thin films treated by 0.5 wt % $CdCl_2$ in methanol, heated in the reaction chamber at 300°C at 10^{-5}Torr with vacuum heat treatment times:1, 2 and 4 min; and following a heat treatment at 500°C for 15 min in the air.

times min	*Z* nm	*Ra* nm	*RMS* nm	R_{p-v} nm	S_{sk} nm	S_{ku} nm
1	403 ± 16	64.8 ± 2.6	51.7 ± 1.8	232 ± 9	-0.4431	3.5394
2	331 ± 13	58.0 ± 2.3	47.2 ± 1.7	195 ± 8	-0.0362	2.443
4	359 ± 14	60.3 ± 2.4	48.2 ± 1.7	175 ± 7	0.3789	2.6787

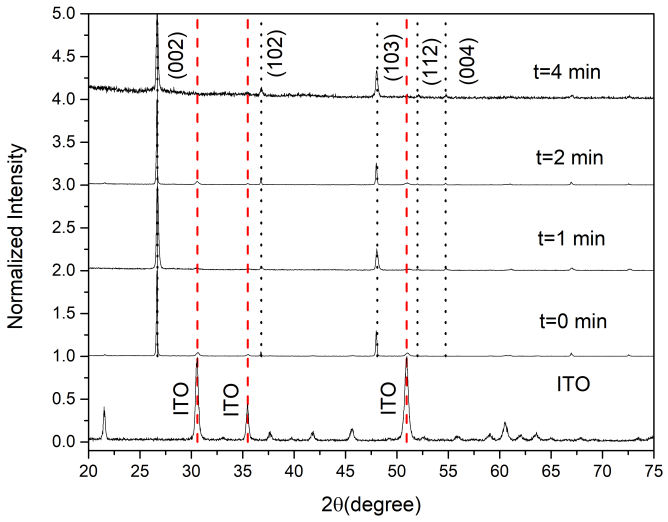

Figure 4. XRD of ITO substrate, the as grown CdS films and treated by 0.5 wt %$CdCl_2$ in methanol heated in the reaction chamber at 300°C at 10^{-5}Torr using times (1, 2 and 4 min) and following a heat treatment at 500°C for 15 min in the air.

During the $CdCl_2$ vacuum heat treatment, there was an increase of stored energy in the crystal defects with time due to the chlorine incorporates into CdS films [36, 37]. We suggest that the mechanism of the recrystallization could be different for each time. For 1 min, the mechanism could take into account as major effect the migration of a pre-existing grain boundary toward the interior of a more highly strained grain and adsorbs stored energy from the local disorderliness created by chlorine. For 2 min, the number of defects must increase with respect to 1 min, in this manner, the crystal defects are surrounded by boundaries provoking grains sub-division, which could be interpreted as a new nucleation center. For 4 min, the grain should be capable of growing at the expense of its neighbors by thermally assisted grain boundary migration. In this way, a decrease in stored energy will occur during heat treatment due to the removal and rearrangement of microstructural defects increasing energy and mobility of the grain boundaries.

Figure 4 displays the XRD patterns of ITO substrate, the as grown CdS films and treated by $CdCl_2$ for 1, 2, and 4 min. The reflections detected reveal that all samples crystallize in the hexagonal structure for polycrystalline CdS [38]. The most intense peak corresponded to the crystalline plane (002) at 26.7°.

The crystallite size of each pattern was estimated using the Williamson−Hall method [39]. The crystalline silicon has been used as a standard reference material for position calibration and instrumental broadening calculation. The full width at half maximum (FWHM) of the peaks (002), (102), (103) and (112) were estimated using the Voigt nonlinear curve fitting function, which gives the best fit for the experimental data. Table III.3 shows 2θ, *FWHM*, the crystallite size for each vacuum heat treatment time. It clearly displays that the behavior of the crystallite size is very similar to that of *Z*, *Ra* and *RMS* (see Table III.3). The highest values of crystalite size is observed for 1 min and the minimum value for 2 min. This confirmed the assumption that changes of the microstructural defects is correlated with the roughness.

Table 3. 2θ, *FWHM*, crystallite size for the CdS films grown at T_{Sour}=650°C and T_{Sub} =450°C during 2 min and after treated by 0.5 wt %$CdCl_2$ in methanol heated in the reaction chamber at 300°C at 10^{-5}Torr using treatment times (1, 2 and 4 min) and following a heat treatment at 500°C for 15 min in the air.

Treatment times (min)	2θ (°)	*FWHM* (°)	**crystallite size (nm)**
1	26.703±0.001 36.832±0.008 48.078±0.006 51.102±0.019	0.203±0.003 0.309±0.122 0.180±0.006 0.506±1.225	40.98±0.11
2	26.619±0.011 36.764±0.005 48.004±0.004 50.989±0.007	0.091±0.003 0.078±0.005 0.099±0.002 0.335±0.028	9.36±0.05
4	26.674±0.002 36.812±0.013 48.049±0.005 52.088±0.053	0.398±0.003 0.170±0.017 0.157±0.002 0.228±0.164	21.52±0.21

The highest value of the crystallite size is reached by the untreated CdS film, which is of 89.58 ± 0.21 nm. This microstructure should help the recrystallization processes and grain growth.

Figure 5 illustrates the relationship between the *RMS* and crystallite size with vacuum heat treatment times. The minimum crystalline size was of 9.36 nm, which corresponded to the lowest value of the *RMS*, which was of 47.2 nm at 2 min. For this heating time, we have hypothesized that the mobility of grain boundaries is unable to eliminate totally the defects produced by the incorporation of Cl in the films and consequently occurred the division of the grains due to that the grain boundaries surrounding such defects. At 1 min, the highest value of the size crystallite is achieved at 40.98 nm consistent with the more value of the *RMS* of the 51.7 nm. In this case, the recrystallization mechanism takes into account the migration of a pre-existing grain boundaries toward the

neighbor grains (see the micrograph of as grown in Figure 5). At 4 min, the crystalline size increased at 21.52 nm while *RMS* was 48.2 nm. When increasing time until 4 min, increasing energy and mobility of the grain boundaries at the expense of removing and rearrangement of microstructural defects.

The mechanisms of recrystallization changed according to the vacuum heat treatment times. The dominant mechanism depended on the mobility and energy of the grain boundaries and the number of microstructural defects existing in the films. Thus, in some cases the movement of the pre-existing grain boundaries prevailed over the number of defects and in others the number of defects generated nuclei of recrystallization.

The recrystallization process is a function of temperature, treatment time, and initial crystal defects in the film. We concluded that $CdCl_2$ was the decisive factor for this process to happen, and hypothesized that the mechanism responsible for the increase in defects in the films, which triggered the recrystallization, was the incorporation of Cl during the treatment.

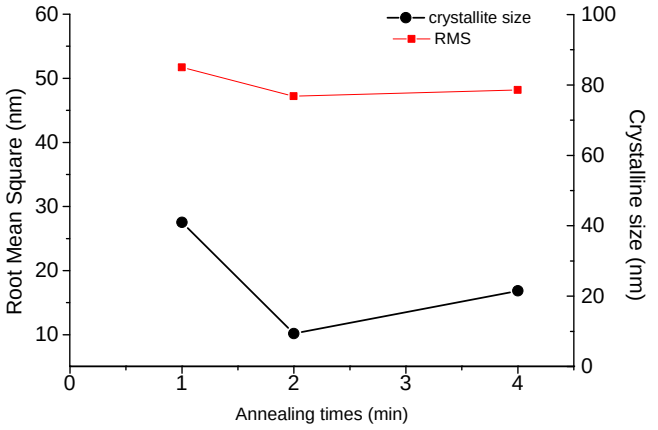

Figure 5. Dependence of the crystallite size, and RMS roughness determined by AFM on the treatment times. (The red line+square symbol correspond to *RMS* and black line+circle to crystallite size).

IV. CONCLUSIONS

Atomic force microscopy (AFM) was employed to monitor surface morphology of CdS thin films prepared on ITO substrates by CSS method and after treated by $CdCl_2$. Based on these results, roughness parameters can lead to a better understanding of recrystallization mechanisms. We have shown the applicability of roughness parameters to describe the effects of the technological process on the surface. We know that our experimental results, based on the recrystallization provoked by $CdCl_2$ treatment, are very similar to those reported by others authors. However, the use of roughness parameters as described in this work could be another option to provides a more comprehensive understanding of the influence of the obtaining conditions on morphological features of the films and could help in tailoring the deposition parameters according to surface morphology requirements for an optoelectronic device applications.

This investigation demonstrated that the roughness parameters can be used to quantify the macroscopic changes that occur on a surface, which are strongly linked with recrystallization processes. The temperature dependence of the growth grain size, the microstructure and the mobility of the border grain can be visualized through the roughness parameters. However, microscopic observations provided evidence that surface roughening of a polycrystalline material is a highly complex process and results from multiple mechanisms. Thus, any prediction about mechanisms or properties of the surface based on the roughness parameters should be carefully planned.

V. ACKNOWLEDGMENTS

We acknowledge funding support from the Programa Nacional de Ciencias Básicas y Naturales (project code PN223LH010-011).

VI. APPENDIX

Roughness Average (*Ra*) used to evaluate the surface roughness, it is described according to:

$$Ra = \frac{1}{N}\sum_{n=1}^{N}|Z_i - \overline{Z}|, \tag{1}$$

$$\overline{Z} = \frac{1}{N}\sum_{i=1}^{N} Z_i \tag{2}$$

Where Z_i is the function that describes the surface profile analyzed in terms of height and position of the sample over the evaluation area.

The *RMS* roughness of a surface is similar to the roughness average, with the only difference being the mean squared absolute values of surface roughness profile. The function *RMS* is defined as:

$$RMS = \frac{1}{N}(\sum_{n=1}^{N}(Z_i - \overline{Z})^2)^{1/2} \tag{3}$$

The *RMS* is more sensitive to peaks and valleys than the average roughness due to the squaring of the amplitude in its calculation.

Maximum height of the profile, R_{p-v}, is defined as the vertical distance between the deepest valley R_v and highest peak R_p.

$$R_{p-v} = R_p - R_v \tag{4}$$

The Skewness (S_{sk}) parameter, which is a 3rd order statistical parameter, used to describe how symmetric a statistical distribution is (namely, when a statistical distribution have S_{sk} values close to zero, we have an almost perfect symmetric height distribution, in other words an almost perfect Gaussian distribution).

The Kurtosis (S_{ku}) parameter, a 4th order statistical parameter used to describe how sharp or how broad a statistical distribution is. Small values of Sku (around value 3) indicate broader height distributions, while values much higher than 3 indicate sharper distributions of peaks on the film surface.

REFERENCES

[1] P. Pfeifer, Appl. Surf. Sci. 18, 146 (1984).

[2] B. Bhushan, Handbook Modern Tribology, (CRC Press, 2001).

[3] E. S. Gadelmawla, M. M. Koura, T. M. A. Maksoud, I. M. Elewa and H. H. Soliman, J. Mater. Process. Technol. **123**, 133 (2002). .

[4] B. B. Mandelbrot, The Fractal Geometry of Nature, (San Francisco, CA, 1983).

[5] F. Family, and T. Vicsek, Dynamics of fractal surfaces, (World Scientific, 1991).

[6] I. Gupta and B. Ch. Mohanty, Sci. Rep. **6**, 1 (2016).

[7] F. Grigoriev, V. Sulimov and A. Tikhonravov, Adv. Opt. Mater. **7**, 13 (2018).

[8] M. P. Hernández, C. F. and Alonso, A. Martel, and E. Casielles, and V. Rejón, and J. L. Peña, Phys. Stat. Sol. (b) **220**, 209 (2000).

[9] B. Bouaouina, A. Besnard, S. E. Abaidia, A. Airoudj and F. Bensouici, Surf. Coat. Tech. **333**, 32 (2018).

[10] A. Drygała, L. A. Dobrzański, M. Szindler, M. M. Szindler, and M. Prokopiuk vel Prokopowicz, E. Jonda, Int. J. Hydrogen Energ. **41**, 7563 (2016).

[11] N. A. Jahan, Md. Minhaz, U. Karim and M. M. Hossain, Adv. Sci. Technol. Eng. Syst. J. **3**, 213 (2018).

[12] G. Kartopu, A. L. Williams, V. Zardetto, A. K. Gürleka, J. Clayton, S. Jones, W. M. M. Kessels, M. Creatore and S. J. C. Irvine, Solar Energy Mater. Solar Cells . **91**, 78 (2019).

[13] R. Kanmani, N. A. M. Zainuddin, M. F. M. Rusdi, S. W. Harun, K. Ahmed, I. S. Amiri and R. Zakaria, Opt. Fiber Technol. **50**, 183 (2019).

[14] T. Begou, F. Lemarchand and J. Lumeau, Opt. Express. **24**, 20925 (2016).

[15] P. K. Mochahari, F. Singh, and K. C. Sarma, J. Mater. Sci.: Mater. **29**, 582 (2018).

[16] N. Saxena, P. Kumar, V. Gupta and D. Kanjilal, J. Mater. Sci.: Mater. **29**, 11013 (2018).

[17] H. Y. R. Atapattu, D. S. M. De Silva, A. A. Ojo and I. M. Dharmadasa, Fabrication of CdS/CdTe Thin Film Solar Cells via the Technique of Electrodeposition, (Development of Solar Power Generation and Energy Harvesting, 2018).

[18] B. E. McCandless, L. V. Moulton and R. W. Birkmire, Prog. Photovolt. Res. Appl. **5**, 249 (1997).

[19] Z. C. Feng, C. C. Wei, A. T. S. Wee, A. Rohatgi and W. Lu, Thin Solid Films **518**, 7199 (2010).

[20] L. Wan, Z. Bai, Z. Hou, D. Wang, H. Sun and L. Xiong, Thin Solid Films **518**, 6858 (2010).

[21] I. Horcas, R. Fernández, J. M. Gómez Rodríguez, J. Colchero, J. Gómez Herrero and A. M. Baro, Rev. Sci. Inst. **78**, 013705 (2007).

[22] S. Chander and M. S. Dhaka, Mater. Res. Bull. **97**, 128 (2018).

[23] R. Yang, D. Wang, L. Wan and D. Wang, Rsc Adv. **4**, 22162 (2014).

[24] S. N. Alamri, Phys. Stat. Sol. (a) . **200**, 352 (2003).

[25] J. Schaffner, E. Feldmeier, A. Swirschuk, H. J. Schimper, A. Klein and W. Jaegermann, Thin Solid Films **519**, 7556 (2011).

[26] C.Doroody, K. S. Rahman, S. F. Abdullah, M. N. Harif, H. N. Rosly, S. K. Tiong, N. Amin, Results Phys. . **18**, 103213 (2020).

[27] M. Kim, S. Sohn, S. Lee, Solar Energy Mater. Solar Cells . **95**, 2295 (2011).

[28] H. R. Moutinho, R. G. Dhere, M. M. Al-Jassim, D. H. Levi, and L. L. Kazmerski, J. Vac. Sci. Technol. A **17**, 1793 (1999).

[29] J. Quadros, A. L. Pinto, H. R. Moutinho, R. G. Dhere and L. R. Cruz, J. Mater. Sci. **43**, 573 (2007).

[30] S. Chander, M. S. Dhaka, Solar Energy **150**, 577 (2017).

[31] L. Vaillant, N. Armani, L. Nasi, G. Salviati, A. Bosio, S. Mazzamuto, N. Romeo, Thin Solid Films **516**, 7075 (2008).

[32] W. S. Mohamed, M. F. Hasaneen and E. K. Shokr, Mater. Res. Express **4**, 046406 (2017).

[33] M. F. Hasaneen, and W. S. Mohamed, Optik. **160**, 307 (2018).

[34] I. M.Dharmadasa, Coatings. **4**, 282 (2014).

[35] P. R. Rios, F. Siciliano Jr, H. R. Zschommler Sandim, R. L. Plaut, and A. F. Padilha, Mater. Res. **8**, 225 (2005).

[36] T. Sivaraman, V. Narasimman, V. S. Nagarethinam and A. R. Balu, Prog. Nat. Sci-Mater. **25**, 392 (2015).

[37] J. D. Major, Semicond. Sci. Technol. **31**, 093001 (2016).

[38] PDF-ICDD, PCPDFWin Version, International Center for Diffraction Data, ICDD, 2002.

[39] G. K. Williamson and W. H. Hall, Acta Metall. **1**, 22 (1953).